UCRL-JC-130424
Preprint

Physics Design of the DARHT 2nd Axis Accelerator Cell

T. L. Houck, Y-J Chen, C. C. Shang
Lawrence Livermore National Laboratory

L. L. Reginato, S. S. Yu
Lawrence Berkeley National Laboratory

This paper was prepared for submittal to
19th International Linear Accelerator Conference
Chicago, Illinois
August 23-28, 1998

August 19, 1998

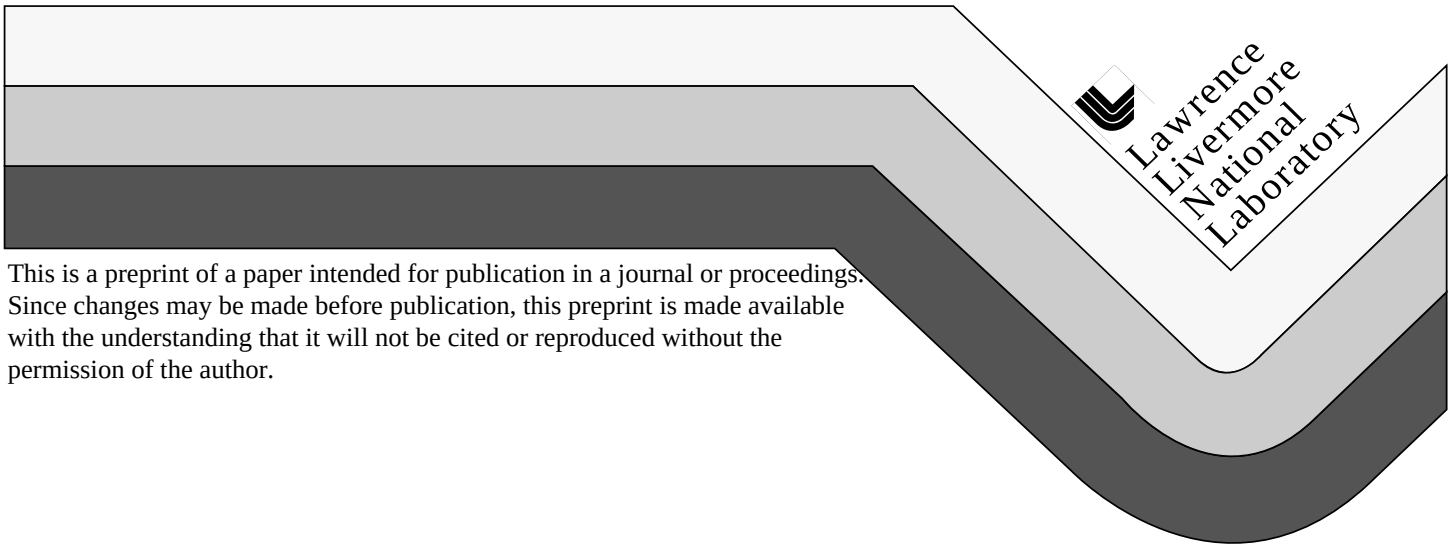

PHYSICS DESIGN OF THE DARHT 2ND AXIS ACCELERATOR CELL*

T.L. HOUCK, Y-J CHEN, and C. SHANG
Lawrence Livermore National Laboratory, Livermore, California 94550 USA
L.L. REGINATO and S.S. YU
Lawrence Berkeley National Laboratory, Berkeley, California 94720 USA

ABSTRACT

The next generation of radiographic machines based on induction accelerators require very high brightness electron beams to realize the desired x-ray spot size and intensity. This high brightness must be maintained throughout the beam transport, from source to x-ray converter target. The accelerator for the second-axis of the Dual Axis Radiographic Hydrodynamic Test (DARHT) facility is being designed to accelerate a 4-kA, 2-μs pulse of electrons to 20 MeV. After acceleration, the 2-μs pulse will be chopped into a train of four 50-ns pulses with variable temporal spacing by rapidly deflecting the beam between a beam stop and the final transport section. The short beam pulses will be focused onto an x-ray converter target generating four radiographic pulses within the 2-μs window. Beam instability due to interaction with the accelerator cells can very adversely effect the beam brightness and radiographic pulse quality. This paper describes the various issues considered in the design of the accelerator cell with emphasis on transverse impedance and minimizing beam instabilities.

1 INTRODUCTION

A DARHT Second Axis Technology Options Study (TOS) was initiated in September 1996 to determine if advances in technology since the design of the first axis induction accelerator warranted a new design for the second axis. The "Long Pulse" option, an induction accelerator that would produce a 2-μs, 4-kA electron beam pulse that could be divided into several shorter pulses, was eventually selected to be the basis for a new design [1]. A preliminary accelerator cell design for the "Long Pulse" option had been presented to the TOS Committee. This preliminary design evolved into the "initial" design described below as detailed engineering design work and beam transport studies were accomplished.

The principle issues necessitating changes to the preliminary cell design involved the material for the vacuum interface insulator and the transport solenoidal magnet field strengths. The dielectric constant for the current insulator is about three times larger than that for the original insulator. The cross sectional area also changed to accommodate fabrication. These changes altered the rf characteristics of the cell and the mode damping scheme for was revised. A more important issue involved the solenoid fields required to transport the beam from the injector into the accelerator. The growth in the beam's transverse centroid motion (instability) is strongly influenced by the transverse impedance of the cell and the transport solenoids' magnetic field strength. See equation (2). Very low solenoidal fields at the front of the accelerator placed a severe constraint on the maximum impedance.

Nearly half of the transverse motion growth occurred in the first 10% of the accelerator with the preliminary design. Thus, it was decided to increase the cell inner radius to reduce the transverse impedance and alter the gap/insulator design to shift the impedance spectrum for the first eight cells. The new gap/insulator design proved to be more compact longitudinally and offered some mechanical advantages over the initial cell design. This design is now the "current" design described below for the first eight larger bore cells and the main accelerator.

*The work was performed under the auspices of the U.S. Department of Energy by LLNL under contract W-7405-ENG-48, and by LBNL under contract AC03-76SF00098.

2 INITIAL DESIGN

This design evolved directly from the TOS "Long Pulse" design. Improvements were made in vacuum surface field stresses, transverse impedance, fabrication ease, and vacuum integrity. Figure 1 is a schematic of this initial accelerator cell design.

2 .1 General Design Criteria

The cross sectional area of the induction cores was set by the required voltage, V, pulse duration, $\Delta\tau$, and core material: $V \cdot \Delta\tau = \Delta B \cdot A \cdot pf$, where (1)

ΔB is the magnetic flux swing, A is the cross sectional area, and pf is the packing fraction of the core material.

The desired maximum growth in the traverse instability and number of cells was used to estimate the maximum transverse impedance. A minimum inner radius consistent with this impedance was then chosen. The following equations are pertinent [2]:

$$\Gamma = \frac{c}{2}\frac{Z_\perp}{l}\frac{I}{I_o}\int_0^L \frac{dz}{B_z}, \text{ and} \qquad (2)$$

$$Z_\perp = 120\frac{W}{r_p^2}\eta \ (\Omega/\text{m}), \text{ where} \qquad (3)$$

Γ is the number of e-folds of growth, $Z_\perp$ is transverse impedance, l is the cell longitudinal length, I is beam current, I_o is 17 kA, L is length of the accelerator, B_z is solenoid field strength, r_p is beam pipe radius, W is cell gap width, and η is a form factor of order unity.

Note that W is approximately the total energy gain of the accelerator divided by number of induction cells and maximum vacuum surface electric field stress. Constraints on the length of the accelerator limited flexibility in determining the outer radius of the induction core.

Determining the optimum B_z involves simulating the beam transport from source to x-ray converter and requires information on expected current and energy variation, location/alignment of components, and cell impedance. This process requires several iterations as the accelerator design matures. The preliminary design assumed the transport fields would be similar to those planned to be used for the first axis accelerator and a conservative value, 12.7 cm, was chosen for r_p.

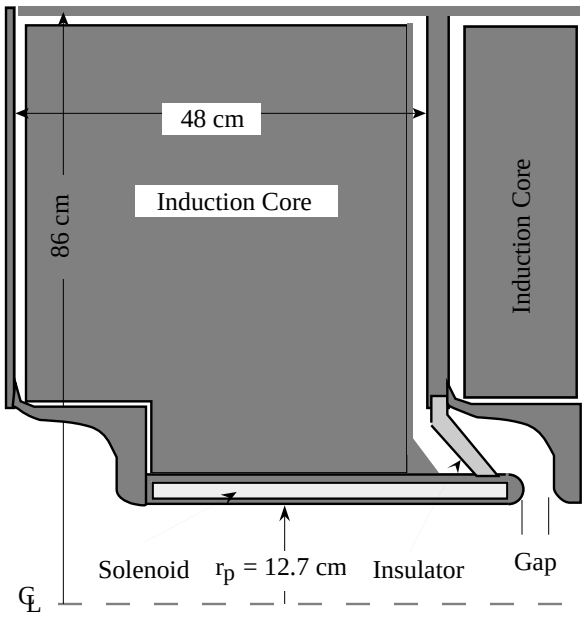

Figure 1. Schematic of the initial accelerator design.

2 .2 Insulator and Field Stress Issues

The insulator has to provide a mechanical interface between the beam line vacuum and the cell insulating oil while withstanding the applied voltage pulse of, in this instance, about 200 kV. It is highly desirable for the insulator to be hidden from line-of-sight view of the beam. See reference [3] for an alternative approach. The simplest design would have been to locate the insulator at the outer radius of the induction cores. Unfortunately, insulating materials, e.g. plastics, that could be fabricated with the required large inner radius, presented an unacceptable gas load due to the large surface area.

A shielded gap design, illustrated in Fig. 2, was used as it permitted the insulator to be placed at a smaller radius (less surface area) while preventing direct line-of-sight with the beam. Rexolite was initially chosen as the insulator material based on performance in operating, short pulse (~100 ns), induction accelerators. However, during long pulse, high-voltage testing performed at LBNL, a Rexolite insulator did not fully recover after experiencing an electrical arc. The insulator was changed to Mycalex to remove any concerns related to insulator performance for long pulses.

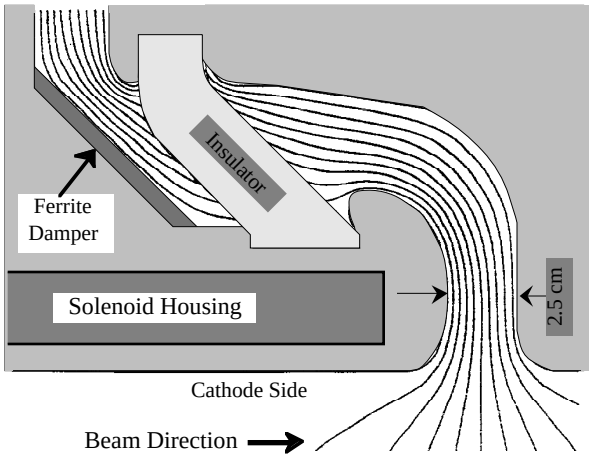

Figure 2. Illustration of the insulator and gap in the initial design. Equipotential lines are shown for the vacuum and oil regions. Each line represents ~20 kV potential change.

Design goals were for vacuum surface electric fields (negative polarity) to be ≤ 100 kV/cm and insulator surface fields ≤ 40 kV/cm. The primary limitation on positive polarity surfaces was to maintain ≤ 100 kV/cm during pulsed power reversals. As the maximum reversed voltage expected is less than 30% of the forward, this was not a difficult requirement. Care was taken to minimize electric fields at triple points (vacuum, metal, and insulator interfaces). Equipotential lines generated by Poisson are shown in Fig. 2 for the vacuum and oil regions of the cell. Maximum fields for the negative polarity (cathode) side of the gap occurred towards the top of the gap nose and were about 100 kV/cm. The maximum field across the insulator occurred towards the top and was about 40 kV/cm. Maximum stress on the positive polarity surfaces was about 130 kV/cm along the curve surfaces approaching the top of the insulator.

2 .3 Transverse Impedance

The transverse impedance of the induction cell was calculated using the AMOS Code [4]. Cell damping was simulated with ferrite, modeled after the TDK PE11B used in the DARHT first axis induction cells, located in the oil region after the insulator as shown in Fig. 2 and on a small section of the outer radius of the core material (not shown). The simulations results are shown in Fig. 3.

3 CURRENT DESIGN

The large radius and low B_z transport fields needed to match the beam from the injector into the accelerator argued for increasing the accelerator bore in the first eight-cell block. Increasing the cell inner radius to 17.8 cm was expected to reduce the impedance by half. See eq. 3.

Desire to reduce the length of the accelerator, while also including more longitudinal space for beam diagnostics, encouraged compactness in the gap/insulator design. The current cell design, shown in Fig. 4, has been adopted for both the larger bore cells and the main accelerator. The notch in the beam pipe wall downstream of the gap is a recess for diagnostics. This design with diagnostic recess has about the same cross section as the initial design.

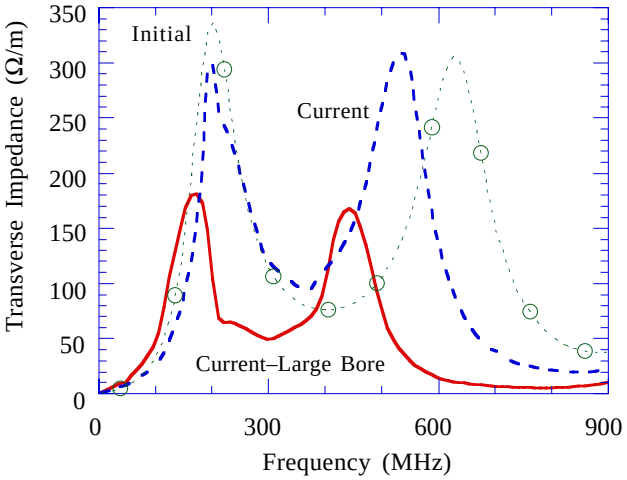

Figure 3. Calculated transverse impedances, $Z_{\perp}$, for the initial and current designs. $Z_{\perp}$ for the first eight larger bore cells using the current design is also shown.

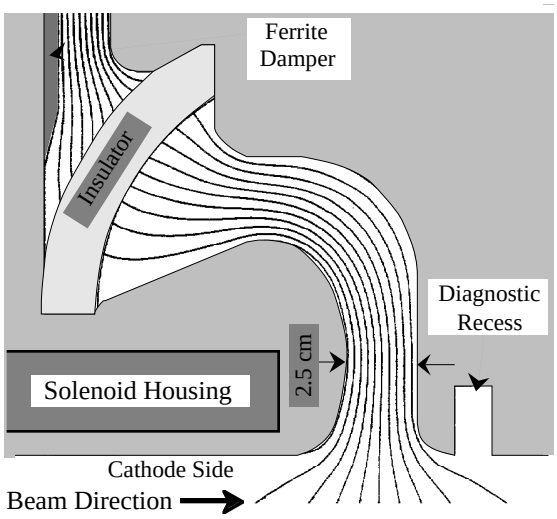

Figure 4. Illustration of the insulator and gap for the current design. Equipotential lines are shown for the vacuum and oil regions. Each line represents ~20 kV potential change.

3 .1 Field Stresses

The first step in arriving at the current design was a series of electrical field stress calculations using Poisson. The current cell design, with equipotential lines plotted, is shown in Fig. 4. The angle of the insulator with respect to the equipotentials was the most significant departure from the initial design with respect to electrical field stress management. Tests with relatively short pulses have determined that the maximum field stress across an insulator can be increased significantly if the electric field makes an angle of 30-45° with respect to the insulator surface [5]. The initial cell design took advantage of this phenomena. It is believed that the field stress in the current design is sufficiently low, < 35 kV/cm for the main accelerator and < 30 kV/cm for the large bore cells, that insulator breakdown will not occur. All conducting surfaces have field stress levels below 100 kV/cm.

3 .2 Transverse Impedance

The transverse impedance of the current induction cell design was also calculated using the AMOS Code and modeling the ferrite damping material as TDK PE11B. The simulations results are shown in Fig. 3. Modest lowering of the impedance can be seen at 200 MHz. The impedance for the larger, 17.8 cm, radius cell is lowered by about half, as expected, and shifted in frequency.

4 SUMMARY

The basic induction cell design for the DARHT second axis accelerator has remained essentially unchanged from the preliminary "Long Pulse" option design. However, the gap/insulator configuration evolved as the engineering design of the accelerator matured, comprehensive beam dynamics simulations were completed, and developmental testing performed. Two gap/insulator configurations have been proposed, a conservative design with respect to the electric field stress on the insulator and a longitudinally compact design. For both configurations, the first eight cells have a larger bore, inner radius of 17.8 cm, than the main accelerator cells, inner radius of 12.7 cm. The compact design is preferred, but the final selection will be made after high-voltage testing of both designs.

5 ACKNOWLEDGMENTS

A very large number of people associated with the DARHT program contributed towards the cell design. In particular, we thank D. Birx, R. Briggs, G. Caporaso, D. Prono, C. Peters, D. Vanecek, and G. Westenskow.

6 REFERENCES

[1] H. Rutkowski, "An Induction Linac for the Second Phase of DARHT," this conference MO2001

[2] Y-J Chen, "Study of the Transverse Beam Motion in the DARHT Phase II Accelerator," this conference TU4033

[3] S. Sampayan, et al., "High-Performance Insulator Structures for Accelerator Applications," Proceedings 1997 Particle Accelerator Conference, (IEEE), New York, N.Y. (1997).

[4] J. Deford, et al., "The AMOS Wakefield Code," *Workshop on Accelerator Computer Codes*, Los Alamos, NM, January 1990.

[5] I. Smith, Proc. First Int. Symp. Discharges and Elec. Insul. in Vac., MIT, Cambridge MA, 1964, p. 261.